

Scrutinizing the Higgs quartic coupling at a future 100 TeV proton-proton collider with taus and b-jets

Benjamin Fuks,^{1,2,3} Jeong Han Kim,⁴ and Seung J. Lee^{5,6}

¹*Sorbonne Universités, Université Pierre et Marie Curie (Paris 06), UMR 7589, LPTHE, F-75005 Paris, France*

²*CNRS, UMR 7589, LPTHE, F-75005 Paris, France*

³*Institut Universitaire de France, 103 boulevard Saint-Michel, 75005 Paris, France*

⁴*Department of Physics and Astronomy, University of Kansas, Lawrence, KS, 66045, USA*

⁵*Department of Physics, Korea University, Seoul 136-713, Korea*

⁶*School of Physics, Korea Institute for Advanced Study, Seoul 130-722, Korea*

(Dated: March 8, 2021)

The Higgs potential consists of an unexplored territory in which the electroweak symmetry breaking is triggered, and it is moreover directly related to the nature of the electroweak phase transition. Measuring the Higgs boson cubic and quartic couplings, or getting equivalently information on the exact shape of the Higgs potential, is therefore an essential task. However, direct measurements beyond the cubic self-interaction of the Higgs boson consist of a huge challenge, even for a future proton-proton collider expected to operate at a center-of-mass energy of 100 TeV. We present a novel approach to extract model-independent constraints on the triple and quartic Higgs self-coupling by investigating triple Higgs-boson hadroproduction at a center-of-mass energy of 100 TeV, focusing on the $\tau\tau b\bar{b}b\bar{b}$ channel that was previously overlooked due to a supposedly too large background. It is thrown into sharp relief that the assist from transverse variables such as m_{T2} and a boosted configuration ensures a high signal sensitivity. We derive the luminosities that would be required to constrain given deviations from the Standard Model in the Higgs self-interactions, showing for instance that a 2σ sensitivity could be achieved for an integrated luminosity of 30 ab^{-1} when Standard Model properties are assumed. With the prospects of combining these findings with other triple-Higgs search channels, the Standard Model Higgs quartic coupling could in principle be reached with a significance beyond the 3σ level.

1. INTRODUCTION

The discovery of a Higgs boson at the Large Hadron Collider (LHC) accomplished the long waited physics goals of getting hints on the nature of the electroweak symmetry breaking (EWSB) mechanism and understanding the generation of the fermion masses. While the discovered Higgs boson appears to be highly compatible with the Standard Model (SM) expectation [1], current data is still insufficient for revealing the true nature of the EWSB dynamics. Further pieces of information related to the shape of the Higgs potential are indeed needed, such as measurements of the Higgs cubic, quartic and even higher-order self-couplings. This would furthermore allow us to investigate whether the electroweak phase transition is of the first or second order, a fact related to the matter-antimatter asymmetry in the universe as a strong first order electroweak phase transition can potentially realize one of the Sakharov conditions for baryogenesis. Measuring the Higgs cubic and quartic self-couplings is consequently one of the major physics goals of the future high-energy physics program.

Di-Higgs production via gluon fusion offers the first playground to access the Higgs cubic coupling, in particular within the high-luminosity phase of the LHC expected to collect an integrated luminosity of 3 ab^{-1} of data at a center-of-mass energy of 14 TeV [2, 3]. The associated sizable (SM) production cross section of about 43 fb [4] allows one to make use of various final states to probe the Higgs cubic coupling, the two most promising

signatures relying on final state systems made of four b -jets, or of a pair of photons and either a pair of b -jets or tau leptons [5–7]. At a future proton-proton collider aiming to operate at a center-of-mass energy of 100 TeV, the $b\bar{b}\gamma\gamma$ channel keeps its leading role and measurements at a precision of about $3 - 4\%$ could be expected for a luminosity of 30 ab^{-1} [8, 9]. None of these searches are, however, designed to probe the Higgs quartic coupling.

In the SM, triple-Higgs production mostly arises, at the leading-order in QCD, by gluon fusion (see Fig. 1). Such a process faces a rather grim prospect at the LHC, mainly because of a small signal rate of $\mathcal{O}(0.1) \text{ fb}$ [10–12], so that the study of this process is left to the experimental program of the post-LHC era that is currently under discussion at CERN and IHEP [13]. Feasibility analyses have so far shown that the $b\bar{b}b\bar{b}\gamma\gamma$ channel can be used to constrain the size of the quartic Higgs coupling in a model-independent way, the interaction strength being allowed to deviate by a factor of at most $\mathcal{O}(10)$ from the SM after considering an integrated luminosity of 30 ab^{-1} [14–16]. The prospects of the $b\bar{b}WWWW$ decay mode have also been explored, and it was shown that a new physics triple-Higgs signal is in principle detectable [17].

In this article, we embark on reinvestigating triple Higgs production at a 100 TeV proton-proton collider to be more confident on the sensitivity of such a machine to the quartic Higgs self-coupling. We focus on the more challenging, branching-ratio-enhanced, $b\bar{b}b\bar{b}\tau^+\tau^-$ signature. Contrary to the $b\bar{b}b\bar{b}\gamma\gamma$ channel, it receives a severe background contamination that yields a weaker expected

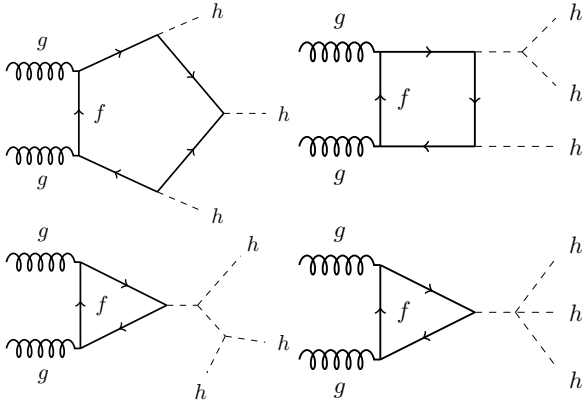


FIG. 1: Representative leading-order Feynman diagrams for triple Higgs production in proton-proton collisions.

sensitivity [14]. However, with the effort of exploiting previously overlooked advantages of the ditau system and a boosted configuration, we show in this work that the $b\bar{b}b\bar{b}\tau\tau$ channel can be promoted to a leading discovery channel for triple-Higgs production.

This paper is organized as follows. In Sec. 2, we introduce the adopted simplified model parameterizing in a model-independent way any new physics effect on the Higgs self-interactions, and we present technical details related to our simulation setup. Sec. 3 is dedicated to our event selection strategy and exhibits details on its specificity. Our results are given in Sec. 4, together with prospects for a future 100 TeV proton-proton colliders.

2. THEORETICAL FRAMEWORK AND TECHNICAL DETAILS

In order to probe for possible new physics effects in multiple-Higgs interactions, we modify in a model-independent fashion the SM Higgs potential,

$$V_h = \frac{m_h^2}{2}h^2 + (1 + \kappa_3)\lambda_{hhh}^{\text{SM}}vh^3 + \frac{1}{4}(1 + \kappa_4)\lambda_{hhhh}^{\text{SM}}h^4,$$

by introducing two κ_i parameters that vanish in the SM. In our notation, h denotes the physical Higgs-boson field, m_h its mass and v its vacuum expectation value. The SM self-interaction strengths moreover read

$$\lambda_{hhh}^{\text{SM}} = \lambda_{hhhh}^{\text{SM}} = \frac{m_h^2}{2v^2}.$$

We simulate our triple Higgs signal and the associated backgrounds by implementing the above Lagrangian in the FEYNRULES package [18] that we use along with the NLOCT program [19] to generate a UFO library [20]. The latter allows for event generation for both tree-level and loop-induced processes within the MADGRAPH5_aMC@NLO [21, 22] framework, that we use to convolute hard scattering matrix elements with the next-to-leading (NLO) set of NNPDF 2.3 parton densities [23] for a center-of-mass energy of $\sqrt{s} = 100$ TeV.

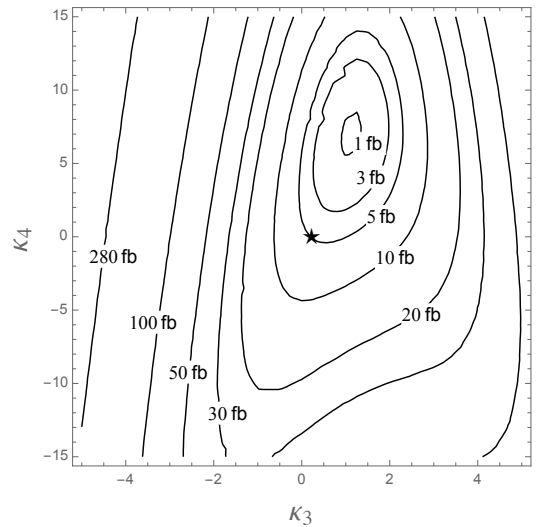


FIG. 2: Triple-Higgs production cross-section for a center-of-mass energy of $\sqrt{s} = 100$ TeV presented as a function of the κ_3 and κ_4 parameters depicting the possible deviations from the SM (indicated by a black star). The results include a conservative NLO K -factor of 2.

The hard-scattering events are then decayed, showered and hadronized within the PYTHIA 6 environment [24] and reconstructed by using the anti- k_T algorithm [25] as implemented in FASTJET [26], with a radius of $R = 1$ and 0.4 for a fat jet and slim jet definition, respectively.

Hadronic taus are defined as specific slim jets for which there is no hadronic object of $p_T > 1$ GeV and no photon with a $p_T > 1.5$ GeV at an angular distance of the jet axis greater than $r_{\text{in}} = 0.1$ and smaller than $r_{\text{out}} = 0.4$. The resulting tau-tagging efficiency is of about 50%, for a fake rate of mistagging a light-flavor jet as a tau of roughly 5%. Those performances can be compared to what could be expected from the high-luminosity phase of the LHC, for which an efficiency of 55% can be expected for a mistagging rate of 0.5% [7].

Our analysis relies on the reconstruction of boosted Higgs bosons. To this aim, we employ the template overlap method [27, 28] as embedded in the TEMPLATETAGGER program [29], and we use a new template observable derived from the ty quantity proposed in Ref. [30], which we here maximize over the different three-body Higgs templates. We make use of various two-body and three-body (NLO) Higgs templates featuring a sub-cone size of 0.1 to compute the discriminating overlaps OV_2^h and OV_3^h , respectively, that allow for a boosted Higgs boson identification. The performance of the method yields a tagging efficiency of 40% for a mistagging rate of 2%.

As suggested by the representative Feynman diagrams of Fig. 1, triple-Higgs production depends on both κ_i parameters as well as on the top Yukawa coupling. While in either an effective field theory framework or an ultraviolet-complete model building approach, the κ_i parameters are not independent, they will be varied in-

Class	Backgrounds	Cross section [ab]
t/W samples	$t_\tau \bar{t}_\tau h_{b\bar{b}}$	2.3×10^4
	$t_\tau \bar{t}_\tau Z_{b\bar{b}}$	6.6×10^3
	$t_\tau \bar{t}_\tau b\bar{b}$	4.7×10^5
	$W_\tau^+ W_\tau^- b\bar{b}b\bar{b}$	4.7×10^5
	$t\bar{t}t\bar{t}$	6.6×10^4
$X_{\tau\tau} + \text{jets}$	$X_{\tau\tau} b\bar{b}b\bar{b}$	6.9×10^4
	$X_{\tau\tau} b\bar{b}jj$	1.5×10^7
	$X_{\tau\tau} t_h \bar{t}_h$	1.6×10^5
	$X_{\tau\tau} Z_{b\bar{b}} b\bar{b}$	2.0×10^3
	$Z_{\tau\tau} h_{b\bar{b}} b\bar{b}$	300
	$X_{\tau\tau} Z_{b\bar{b}} Z_{b\bar{b}}$	23
	$Z_{\tau\tau} h_{b\bar{b}} Z_{b\bar{b}}$	15
	$h_{\tau\tau} h_{b\bar{b}} Z_{b\bar{b}}$	11
Di-Higgs	$h_{b\bar{b}} h_{b\bar{b}} Z_{\tau\tau}$	
	$h_{\tau\tau} h_{b\bar{b}} + \text{jet}$	1.3×10^3

TABLE I: Fiducial cross sections of all components of the SM background after the baseline selection described in Sec. 3. The results include an NLO K -factor of 2, and the suffixes ‘ τ ’ and ‘ $b\bar{b}$ ’ respectively indicate decays into a tau-lepton and a $b\bar{b}$ pair, t_h denoting similarly a hadronically-decaying top quark.

dependently in our study. Moreover, the top Yukawa coupling is assumed to be fixed to its SM value. The resulting production cross section is presented in Fig. 2 in the (κ_3, κ_4) plane after including a flat NLO K -factor of 2 [31]. The sign of the κ_3 parameter turns out to be crucial due to respective constructive and destructive interference patterns when κ_3 is negative and positive. As a consequence, the cross section can be reduced to below the fb level when both κ parameters are positive (and not too large), making this corner of the parameter space hard to probe. The variations in κ_4 are in addition mild for any fixed value of κ_3 , so that only poor constraints could be expected from any potential measurement.

Among all triple-Higgs production signatures, we make use of the $b\bar{b}b\bar{b}\tau^+\tau^-$ channel with two hadronic tau decays to probe deviations in the Higgs self-interactions. Whilst the branching ratio is large ($\sim 6.3\%$), the background contamination is expected to be important [14]. We however demonstrate in the next sections that previously overlooked advantages stemming from the usage of specific kinematic properties of the ditau systems and the potentially boosted configuration of the b -jet pairs could largely increase the signal significance.

The various components of the SM background can be classified into three categories regarding their response to the basic selection criteria introduced in Sec. 3. We denote by t/W samples the ensemble of background processes featuring a top quark or a W -boson pair that decays into a tau-enriched final state, together with the four-top background contributions. The second class of SM backgrounds consists of the $X_{\tau\tau} + \text{jets}$ category with X being a virtual photon, Higgs or Z -boson decaying

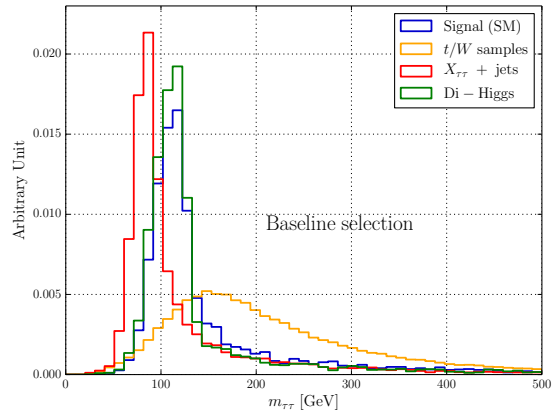


FIG. 3: Distribution in the $m_{\tau\tau}$ invariant mass (as defined in the text) after the baseline selection for the three SM background categories and for a SM triple-Higgs signal.

into a pair of tau leptons. Di-Higgs production in association with jets finally forms the last class of background processes on its own. The full list of considered SM backgrounds is summarized in Table I, where we additionally present the fiducial cross sections, multiplied by a conservative NLO K -factor of 2, obtained after requiring the presence of two hadronic taus and missing transverse energy (*cf.* the baseline selection described in Sec. 3).

3. SIGNAL SELECTION

Our triple-Higgs analysis relies for its baseline selection on the properties of the $b\bar{b}b\bar{b}\tau^+\tau^-$ final state. We preselect events featuring exactly two hadronic taus with a $p_T > 25$ GeV and a pseudorapidity $|\eta| < 2.5$, as well as a missing transverse energy $\cancel{E}_T > 25$ GeV.

After this preselection, the two taus are enforced to be compatible with the decay of a Higgs boson by means of the $m_{\tau\tau}^{\text{Higgs-bound}}$ and m_T^{True} variables [32–34]. The former quantity is defined by minimizing, over all possible assignments for the neutrino four-momenta, the invariant mass of the system made of the two tau jets and the two invisible neutrinos. This minimization procedure however requires that each tau jet is matched with a neutrino and that the resulting two-body invariant mass is compatible with the tau mass. For cases for which there is no such a solution, the m_T^{True} variable is constructed instead in the same way, but without this last constraint. We present the resulting $m_{\tau\tau}$ distribution in Fig. 3, $m_{\tau\tau}$ generically denoting $m_{\tau\tau}^{\text{Higgs-bound}}$ when it can be constructed and m_T^{True} otherwise. Most signal events exhibit an $m_{\tau\tau}$ value lying between the Z and the Higgs boson masses, whereas background events from the $X_{\tau\tau} + \text{jets}$ category mainly feature smaller $m_{\tau\tau}$ values. We therefore impose that $m_{\tau\tau} \in [105, 135]$ GeV to ensure compatibility with a Higgs ditau decay and a very good

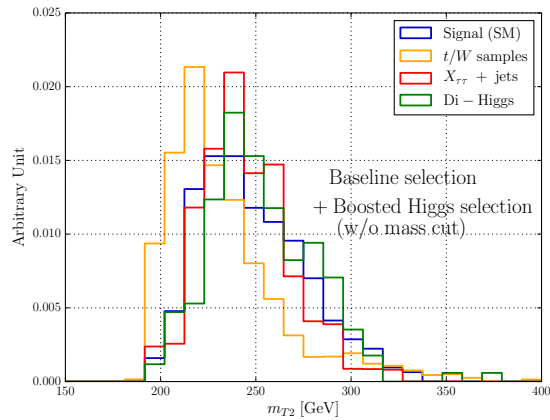


FIG. 4: m_{T2} spectra for the signal (in the case of a SM Higgs potential) and the various components of the background.

discrimination from the $X_{\tau\tau} + \text{jets}$ background category.

We move on with the reconstruction of the two other Higgs bosons for which we rely on a configuration where one of them is boosted and the other one is resolved. We select events featuring at least one fat jet whose basic properties satisfy $p_T > 300$ GeV and $|\eta| < 2.5$. The fat jet invariant mass is moreover required to lie in the $[105, 135]$ GeV window and the template overlaps are constrained to $OV_3^h > 0.7$ and $OV_2^h > 0.2$. We additionally require the presence of at least two slim jets and tag two of them as candidates for a non-boosted Higgs decay. This tagging is such that the dijet invariant mass $m_{jj} \in [105, 135]$ GeV minimizes $|m_{jj} - m_h|$. Furthermore, one of the two tagged slim jets must be b -tagged and the fat jet must contain a doubly- b -tagged substructure when we assume a b -tagging efficiency of 70% when a B -hadron is present in a cone of radius $R = 0.4$ around the jet direction, for a corresponding mistagging rate of 1%.

At this stage, the background is dominated by its t/W component (see Table II). In contrast to the triple-Higgs signal in which the missing energy originates from the two neutrinos associated with the tau decays, most background events feature either more than two neutrinos, or a missing energy originating from a W -boson pair. This suggests to take advantage of the m_{T2} variable [35, 36] to ensure an efficient background rejection. The m_{T2} spectrum is bounded from above and its shape depends both on a test mass and on the mass of the semi-invisibly decaying particle. Moreover, the upper bound sharply rises for increasing test masses above the true mass of the invisible particle [37]. As the true invisible mass is zero for the triple Higgs signal, the associated m_{T2} distribution is naturally broader than for the background, provided the test mass is taken large enough. This feature is illustrated in Fig. 4 for which we have chosen an optimized test mass of 190 GeV, which allows for a maximal background and signal separation.

Selection	Signal	t/W	$X_{\tau\tau}$	hh
Baseline	27	1.0×10^6	1.6×10^7	1.3×10^3
$m_{\tau\tau}$	12	1.4×10^5	2.6×10^6	670
Boosted Higgs	0.92	640	6.5×10^3	35
m_{jj}	0.47	180	81	4.1
b -tagging	0.15	15	0.20	0.034
m_{T2}	0.11	0.37	0.093	0.029
m_{hhh}	0.10	8.5×10^{-3}	0.012	0.026
S/B	2.1			
σ	2.0			

TABLE II: Signal and background cross sections, in ab , at different stage of the analysis strategy depicted in Sec. 3. The signal to background ratio S/B and the significance σ for a luminosity of 30 ab^{-1} are also indicated.

After having reconstructed all three Higgs bosons, we derive the invariant mass of the triple-Higgs system m_{hhh} and constrain it to be smaller than 1.6 TeV.

4. RESULTS AND DISCUSSION

We present in Table II the fiducial cross sections resulting from the application of the various selections introduced in Sec. 3, both for the signal (assuming the SM case with $\kappa_3 = \kappa_4 = 0$) and the background. We can observe the complementarity of the various steps, the $m_{\tau\tau}$ and boosted Higgs requirements reducing the background by a factor of more than 2000, while the reconstruction of the resolved Higgs boson and the b -tagging conditions bring the signal over background (S/B) ratio down to the percent level. The background is at this stage dominated by t/W events and is further reduced to a manageable level by means of the m_{T2} selection. The selection on the triple-Higgs invariant mass finally brings the background rate to half the signal one for the considered benchmark.

In order to set limits and derive the future collider sensitivity in the (κ_3, κ_4) plane, we compute a significance σ defined as the likelihood ratio [38]

$$\sigma \equiv \sqrt{-2 \ln \left(\frac{L(B|S+B)}{L(S+B|S+B)} \right)} \text{ with } L(x|n) = \frac{x^n}{n!} e^{-x},$$

where S and B are the expected number of signal and background events respectively. The signal sensitivity turns out to be of about 2σ in the SM case for a luminosity of 30 ab^{-1} , with a number of signal events $S \sim 3$ and background events $B \sim 1.4$. The number of signal events could however be increased by considering the strategic approach of including the contributions of a semi-leptonic $\tau_h \tau_l b \bar{b} b \bar{b}$ final state, as it has been recently proposed for di-Higgs searches at the LHC [7].

Scanning over the κ_i parameters, we show in Fig. 5 the luminosity goals of a 100 TeV proton-proton collider necessary for achieving a 2σ exclusion (left panel). Despite

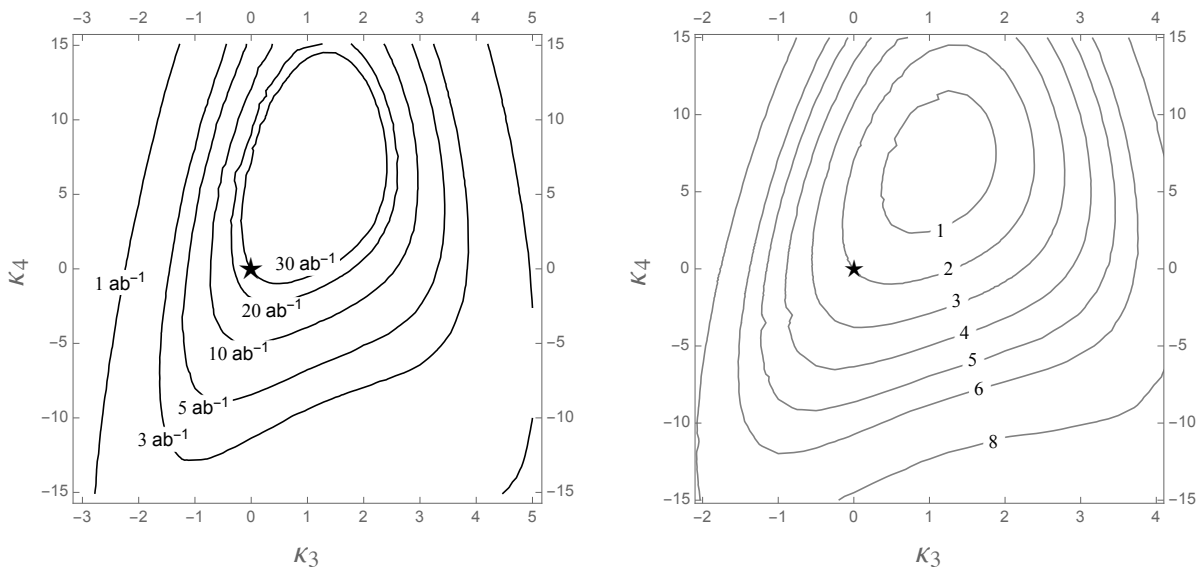


FIG. 5: Minimum luminosity of 100 TeV proton-proton collisions required to achieve a 2σ sensitivity to a triple-Higgs signal in the $bbb\bar{\tau}\bar{\tau}$ channel shown in terms of the κ_3 and κ_4 parameters (left), and the corresponding sensitivity expected for a luminosity of 30 ab^{-1} (right).

the dominance of destructive interferences on the upper-right-corner of the (κ_3, κ_4) plane, our analysis demonstrates that the SM expectation can in principle be excluded with 30 ab^{-1} . Conversely, we present in the right panel of the figure the significance contours obtained when considering a luminosity of 30 ab^{-1} . In order to access the sensitivity gap in the parameter space region limited by $\kappa_3 \in [0, 2]$ and $\kappa_4 \in [0, 14]$, one could combine our results with other channels, like the $\tau_h \tau_l b\bar{b}b\bar{b}$ mode that could enhance the sensitivity of the present analysis, and the $\gamma b\bar{b}b\bar{b}$ channel investigated in Refs. [14–16]. Our findings could moreover be merged with the more precise prospects on the κ_3 parameters that stem from di-Higgs probes expected to be produced at a large rate [8, 9].

In this work, we have continued our investigation of the possibilities of a future proton-proton collider expected to run at $\sqrt{s} = 100 \text{ TeV}$ to unravel the true nature of the EWSB mechanism. We have shown that in addition to the $\gamma b\bar{b}b\bar{b}$ golden channel, the $bbb\bar{\tau}\bar{\tau}$ mode is a complementary probe to the quartic Higgs self-interaction. Our results are comparable to those derived in other triple-Higgs channels, so that combinations of several searches could offer handles to parameter space regions featuring low cross sections and not accessible with a single triple-Higgs analysis. Such a combination also gives hope to

access the SM couplings beyond the 3σ level.

Acknowledgements: We are very grateful to Minho Son for valuable help and discussions, in particular on tau reconstruction, as well as to K.C. Kong, Ian M. Lewis and Graham Wilson for useful comments and suggestions during the course of this project. We also thank the HT-CaaS group of the Korea Institute of Science and Technology Information (KISTI) for providing the necessary computing resources and acknowledge the Korea Future Collider Study Group (KFCSG) for motivating us to proceed with this work. JHK is supported in part by US-DOE (DE-FG02-12ER41809) and by the University of Kansas General Research Fund allocation 2302091. SL is supported by the National Research Foundation of Korea (NRF) grant funded by the Korea government (MEST) (No. NRF-2015R1A2A1A15052408), and by the Korean Research Foundation (KRF) through the Korea-CERN collaboration program (NRF-2016R1D1A3B01010529). The work of BF is partly supported by French state funds managed by the Agence Nationale de la Recherche (ANR), in the context of the LABEX ILP (ANR-11-IDEX-0004-02, ANR-10-LABX-63), and by the FKPPL initiative of the CNRS.

[1] **ATLAS, CMS** Collaboration, G. Aad et al., *Measurements of the Higgs boson production and decay rates and constraints on its couplings from a combined ATLAS and CMS analysis of the LHC pp collision data at $\sqrt{s} = 7$ and 8 TeV* , *JHEP* **08** (2016) 045, [[arXiv:1606.02266](#)].

[2] M. J. Dolan, C. Englert, and M. Spannowsky, *Higgs self-coupling measurements at the LHC*, *JHEP* **10** (2012) 112, [[arXiv:1206.5001](#)].
 [3] J. Baglio, A. Djouadi, R. Gröber, M. M. Mühlleitner, J. Quevillon, and M. Spira, *The measurement of the Higgs self-coupling at the LHC: theoretical status*, *JHEP*

- 04 (2013) 151, [[arXiv:1212.5581](#)].
- [4] D. de Florian and J. Mazzitelli, *Higgs pair production at next-to-next-to-leading logarithmic accuracy at the LHC*, *JHEP* **09** (2015) 053, [[arXiv:1505.07122](#)].
- [5] **ATLAS** Collaboration, *Projected sensitivity to non-resonant Higgs boson pair production in the $b\bar{b}b\bar{b}$ final state using proton-proton collisions at HL-LHC with the ATLAS detector*, ATL-PHYS-PUB-2016-024.
- [6] **ATLAS** Collaboration, *Study of the double Higgs production channel $H(\rightarrow b\bar{b})H(\rightarrow \gamma\gamma)$ with the ATLAS experiment at the HL-LHC*, ATL-PHYS-PUB-2017-001.
- [7] **CMS** Collaboration, *Higgs pair production at the High Luminosity LHC*, CMS-PAS-FTR-15-002.
- [8] R. Contino et al., *Physics at a 100 TeV pp collider: Higgs and EW symmetry breaking studies*, [arXiv:1606.09408](#).
- [9] A. Azatov, R. Contino, G. Panico, and M. Son, *Effective field theory analysis of double Higgs boson production via gluon fusion*, *Phys. Rev.* **D92** (2015), no. 3 035001, [[arXiv:1502.00539](#)].
- [10] T. Plehn and M. Rauch, *The quartic higgs coupling at hadron colliders*, *Phys. Rev.* **D72** (2005) 053008, [[hep-ph/0507321](#)].
- [11] T. Binoth, S. Karg, N. Kauer, and R. Ruckl, *Multi-Higgs boson production in the Standard Model and beyond*, *Phys. Rev.* **D74** (2006) 113008, [[hep-ph/0608057](#)].
- [12] F. Maltoni, E. Vryonidou, and M. Zaro, *Top-quark mass effects in double and triple Higgs production in gluon-gluon fusion at NLO*, *JHEP* **11** (2014) 079, [[arXiv:1408.6542](#)].
- [13] N. Arkani-Hamed, T. Han, M. Mangano, and L.-T. Wang, *Physics opportunities of a 100 TeV proton-proton collider*, *Phys. Rept.* **652** (2016) 1–49, [[arXiv:1511.06495](#)].
- [14] B. Fuks, J. H. Kim, and S. J. Lee, *Probing Higgs self-interactions in proton-proton collisions at a center-of-mass energy of 100 TeV*, *Phys. Rev.* **D93** (2016), no. 3 035026, [[arXiv:1510.07697](#)].
- [15] C.-Y. Chen, Q.-S. Yan, X. Zhao, Y.-M. Zhong, and Z. Zhao, *Probing triple-Higgs productions via $4b2\gamma$ decay channel at a 100 TeV hadron collider*, *Phys. Rev.* **D93** (2016), no. 1 013007, [[arXiv:1510.04013](#)].
- [16] A. Papaefstathiou and K. Sakurai, *Triple Higgs boson production at a 100 TeV proton-proton collider*, *JHEP* **02** (2016) 006, [[arXiv:1508.06524](#)].
- [17] W. Kilian, S. Sun, Q.-S. Yan, X. Zhao, and Z. Zhao, *New Physics in multi-Higgs boson final states*, [arXiv:1702.03554](#).
- [18] A. Alloul, N. D. Christensen, C. Degrande, C. Duhr, and B. Fuks, *FeynRules 2.0 - A complete toolbox for tree-level phenomenology*, *Comput. Phys. Commun.* **185** (2014) 2250–2300, [[arXiv:1310.1921](#)].
- [19] C. Degrande, *Automatic evaluation of UV and R2 terms for beyond the Standard Model Lagrangians: a proof-of-principle*, *Comput. Phys. Commun.* **197** (2015) 239–262, [[arXiv:1406.3030](#)].
- [20] C. Degrande, C. Duhr, B. Fuks, D. Grellscheid, O. Mattelaer, and T. Reiter, *UFO - The Universal FeynRules Output*, *Comput. Phys. Commun.* **183** (2012) 1201–1214, [[arXiv:1108.2040](#)].
- [21] J. Alwall, R. Frederix, S. Frixione, V. Hirschi, F. Maltoni, O. Mattelaer, H. S. Shao, T. Stelzer, P. Torrielli, and M. Zaro, *The automated computation of tree-level and next-to-leading order differential cross sections, and their matching to parton shower simulations*, *JHEP* **07** (2014) 079, [[arXiv:1405.0301](#)].
- [22] V. Hirschi and O. Mattelaer, *Automated event generation for loop-induced processes*, *JHEP* **10** (2015) 146, [[arXiv:1507.00020](#)].
- [23] R. D. Ball et al., *Parton distributions with LHC data*, *Nucl. Phys.* **B867** (2013) 244–289, [[arXiv:1207.1303](#)].
- [24] T. Sjostrand, S. Mrenna, and P. Z. Skands, *PYTHIA 6.4 Physics and Manual*, *JHEP* **0605** (2006) 026, [[hep-ph/0603175](#)].
- [25] M. Cacciari, G. P. Salam, and G. Soyez, *The Anti- $k(t)$ jet clustering algorithm*, *JHEP* **0804** (2008) 063, [[arXiv:0802.1189](#)].
- [26] M. Cacciari, G. P. Salam, and G. Soyez, *FastJet User Manual*, *Eur.Phys.J.* **C72** (2012) 1896, [[arXiv:1111.6097](#)].
- [27] L. G. Almeida, S. J. Lee, G. Perez, G. Sterman, and I. Sung, *Template Overlap Method for Massive Jets*, *Phys.Rev.* **D82** (2010) 054034, [[arXiv:1006.2035](#)].
- [28] L. G. Almeida, O. Erdogan, J. Juknevich, S. J. Lee, G. Perez, et al., *Three-particle templates for a boosted Higgs boson*, *Phys.Rev.* **D85** (2012) 114046, [[arXiv:1112.1957](#)].
- [29] M. Backović and J. Juknevich, *TemplateTagger v1.0.0: A Template Matching Tool for Jet Substructure*, *Comput.Phys.Commun.* **185** (2014) 1322–1338, [[arXiv:1212.2978](#)].
- [30] J. H. Kim, K. Kong, S. J. Lee, and G. Mohlabeng, *Probing TeV scale Top-Philic Resonances with Boosted Top-Tagging at the High Luminosity LHC*, *Phys. Rev.* **D94** (2016), no. 3 035023, [[arXiv:1604.07421](#)].
- [31] D. de Florian and J. Mazzitelli, *Two-loop corrections to the triple Higgs boson production cross section*, *JHEP* **02** (2017) 107, [[arXiv:1610.05012](#)].
- [32] A. J. Barr, S. T. French, J. A. Frost, and C. G. Lester, *Speedy Higgs boson discovery in decays to tau lepton pairs: $h\rightarrow\tau,\tau$* , *JHEP* **10** (2011) 080, [[arXiv:1106.2322](#)].
- [33] A. J. Barr, B. Gripaios, and C. G. Lester, *Measuring the Higgs boson mass in dileptonic W-boson decays at hadron colliders*, *JHEP* **07** (2009) 072, [[arXiv:0902.4864](#)].
- [34] A. J. Barr, M. J. Dolan, C. Englert, and M. Spannowsky, *Di-Higgs final states augMT2ed – selecting hh events at the high luminosity LHC*, *Phys. Lett.* **B728** (2014) 308–313, [[arXiv:1309.6318](#)].
- [35] C. G. Lester and D. J. Summers, *Measuring masses of semiinvisibly decaying particles pair produced at hadron colliders*, *Phys. Lett.* **B463** (1999) 99–103, [[hep-ph/9906349](#)].
- [36] A. Barr, C. Lester, and P. Stephens, *$m(T2)$: The Truth behind the glamour*, *J. Phys.* **G29** (2003) 2343–2363, [[hep-ph/0304226](#)].
- [37] A. J. Barr, B. Gripaios, and C. G. Lester, *Weighing Wimps with Kinks at Colliders: Invisible Particle Mass Measurements from Endpoints*, *JHEP* **02** (2008) 014, [[arXiv:0711.4008](#)].
- [38] G. Cowan, K. Cranmer, E. Gross, and O. Vitells, *Asymptotic formulae for likelihood-based tests of new physics*, *Eur. Phys. J.* **C71** (2011) 1554, [[arXiv:1007.1727](#)]. [Erratum: *Eur. Phys. J.* **C73**,2501(2013)].